MULTISENSOR STUDY OF WIND PATTERNS AND ALGAL BLOOMS IN NEAR-COASTAL GYRES OF THE MEDITERRANEAN SEA

Vittorio Barale

Institute for Environment and Sustainability, Joint Research Centre, European Commission
TP 272, Via E. Fermi 2749, I-21027 Ispra (VA), Italy; vittorio.barale@jrc.it

Martin Gade

Zentrum für Meeres- und Klimaforschung, Institut für Meereskunde, Universität Hamburg
Bundesstraße 53, D-20146 Hamburg, Germany; martin.gade@zmaw.de

ABSTRACT

QuikScat and SeaWiFS data (2000-2007) covering the Mediterranean Sea were used for a multisensor study of the coupling between wind patterns and algal blooms in the Gulf of Lion and the Rhodes-Ierapetra gyre systems. In these near-coastal hotspots, atmospheric forcing creates (albeit with different mechanisms) surface conditions that cause convective processes and consequent nutrient upwelling from deeper layers. As phytoplankton growth in the otherwise oligotrophic Mediterranean basin is always nutrient-limited, the blooming triggered by these processes reflects the prevailing wind patterns. Highly dynamic features recur systematically in the pigment field of both regions, in the same periods (January to May).

Keywords: Mediterranean Sea, SeaWiFS, QuikScat, algal blooms, sea winds, gyres

INTRODUCTION

The combined use of sundry remote sensing tools, to assess complementary environmental data, provides novel opportunities for the assessment of coastal and marine processes. A comparison of QuikScat and of Sea-viewing Wide Field-of-view Sensor (SeaWiFS) data, for the period 2000-2007, was used to study the coupling between wind patterns and algal blooms in two regions of the Mediterranean Sea: the Ligurian-Provençal Sea, from 40 to 44°N, 2 to 8°E, and the Levantine Basin, from 32 to 38°N, 24 to 32°E (Figure 1).

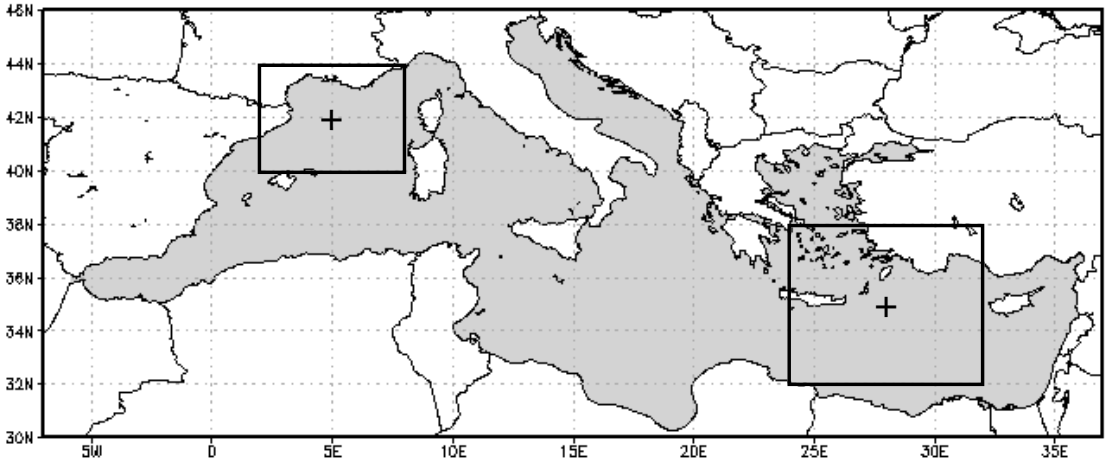

Figure 1: Mediterranean Sea, areas of interest: Ligurian-Provençal Sea (upper left box, centred at 42°N, 5°E) and Levantine Basin (lower right box, centred at 35°N, 28°E).

The Mediterranean Sea is predominantly oligotrophic and behaves like a sub-tropical basin, where the light level is never a limiting factor, so that its decrease in winter does not inhibit algal growth, but the nutrient level always is. Blooming occurs in the colder, windy and wet (winter) season, and is related to the biological enrichment of surface waters due to cooling,

vertical mixing and continental runoff, but not in the warmer, calm and dry (summer) season, when the water column is strongly stratified and the nutrient supply, from coastal zones or deeper layers, is much reduced (i).

Oligotrophy increases from west to east, except for near-coastal hotspots, corresponding to point sources of runoff (often affected by a severe anthropogenic impact) or to areas where atmospheric forcing creates particular conditions that favour the blooming. This is the case of near-coastal features such as the Lions Gyre and the Ierapetra-Rhodes Gyre system (see Figure 2). In both areas, bloom dynamics reflect enhanced air-sea interactions due to the prevailing wind patterns (i.e. the Mistral and the Etesian winds, respectively). In the north-western basin, the northerly wind increases the density of surface waters through intense evaporation and cooling, particularly in the Gulf of Lions, and generates deep convection processes (ii). This can lead to a complete overturning of the water column, thus ventilating the deepest parts of the basin and bringing deep nutrient-rich waters to the surface. When the water column stabilizes, this favours the onset of intense algal blooms. In the south-eastern basin, northerly winds blowing along the axis of the Aegean Sea funnel through the straits between the Islands of Crete and Rhodes, generating a (quasi) permanent vortex pair (ii). This comprises the cyclonic Rhodes Gyre, north-east of the straits, and the anticyclonic Ierapetra Gyre, south-west of the straits – often entrained in the complex basin-wide surface circulation of the eastern Mediterranean (iii). In the first case, the divergence due to Ekman pumping is linked to the upwelling of colder, nutrient-rich waters; in the second, the convergence is linked to the accretion and downwelling of warm, nutrient-poor surface waters.

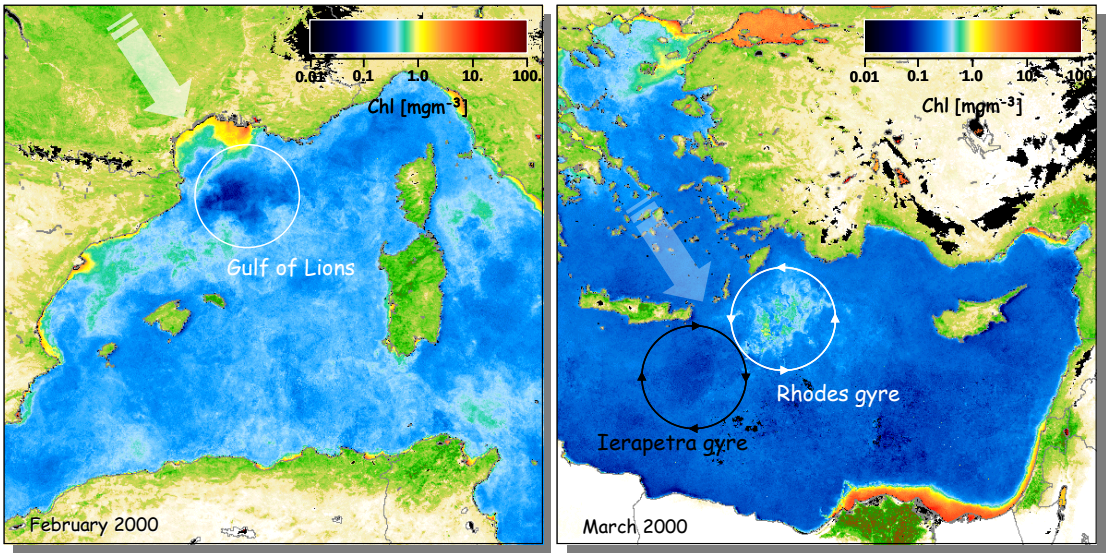

Figure 2: Monthly means of SeaWiFS-derived (iv) chlorophyll-like pigment concentration [mg/m^3], and a land vegetation index – the Fraction of Absorbed Photosynthetically Active Radiation, FAPAR – in the Ligurian-Provençal Sea (left panel), February 2000, and in the Levantine Basin (right panel), March 2000. Both images cover an area of about 1000 km x 1000 km, with 2 km spatial resolution. The circles indicate sites of deep convection, in the Gulf of Lion, and of upwelling/downwelling, in the Rhodes-Ierapetra gyre system. The large arrows recall the prevailing wind patterns.

THE QuikScat AND SeaWiFS DATA SET

The wind speed data were collected by the microwave scatterometer SeaWinds, which was launched on the QuikBird satellite in June 1999. The QuikBird SeaWinds, later dubbed QuikScat, is the third in a series of NASA scatterometers that operate at 14 GHz (Ku-band). Scatterometers transmit microwave pulses down to the Earth's surface and then measure the power that is scattered back to the instrument, and that is related to surface roughness. For water surfaces, the surface roughness is highly correlated with the near-surface wind speed and direction (v, vi). Hence, wind speed and direction at a height of 10 meters over the ocean surface can be retrieved from measurements of the scatterometer's backscattered power. The 2000-2007 data used here, for comparison with the SeaWiFS data, are mapped to a 0.25 degree grid. Overlaid to the colour-coded maps of wind speed are black arrows denoting the

mean surface wind direction, on a 0.5 degree grid. The wind speeds represent scalar averages of daily data, while the wind directions are vector averages of the same data[1].

The chlorophyll-like pigment concentration (*Chl*) data were collected by the visible and near infrared radiometer SeaWiFS, which was launched on the SeaStar satellite in September 1997. The original imagery was processed[2] to correct top-of-the-atmosphere radiances from atmospheric noise, to derive normalized water-leaving radiances, and then to compute from these a series of derived parameters (including C*hl*). Except for the pictures shown in Figure 2 (see Figure caption for details), each daily image of the 2000-2007 dataset was treated using the SeaDAS algorithm set (vii) and re-mapped on a common equal-area grid, with a grid cell, or "bin", of 9 km x 9 km. For the creation of the composite data products, all valid pixels of a given time period and grid cell were compiled in the same bin, and their weighted mean was generated. The weight was based on the number of valid pixels used in the binning process (viii). Single images at full resolution (~1.2 km at nadir) display a larger amount of details, but are often incomplete over areas of the size considered here, due to imaging geometry, algorithm failure or cloud cover, even with daily overpasses of a wide-swath sensor. Hence the choice of utilizing composite images to assess the main *Chl* patterns from a statistical point of view. Because the number of valid pixels increases with larger and longer binning intervals, the compositing process generates complete, cloud-free images. As will be seen in the following, though, the short-term variability is averaged out too, and the composites retain only those patterns that persist over significant areas and periods of time.

WIND PATTERNS AND ALGAL BLOOMS

The seasonal and multi-annual trends of the average wind speed and *Chl* values, computed in the Ligurian-Provençal Sea and the Levantine Basin domains[3] shown in Figure 1, during the period considered (January 2000 to April 2007), are shown in Figure 3. The wind speed record shows that maxima are reached systematically in the fall-winter period, i.e. between October and March. Conversely, the *Chl* record peaks in January-February, for the Levantine Basin, and even later, in March-April, for the Ligurian-Provençal Sea.

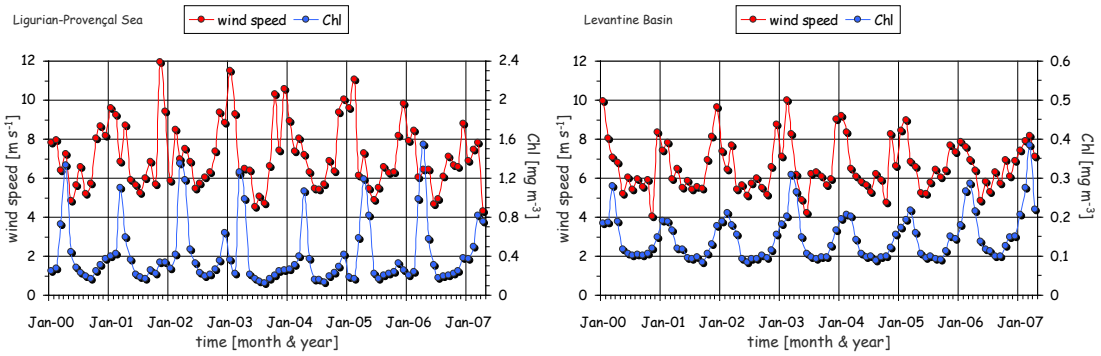

Figure 3: Monthly mean wind speed and Chl in the Ligurian-Provençal Sea (left panel) and in the Levantine Basin (right panel).Note the different Chl scale, on the right vertical axis.

Examples of the surface wind fields in the two areas considered are shown in panels (a) and (c) of Figure 4. The corresponding surface pigment fields are shown in panels (b) and (d) of the same Figure. In both cases, the image series comprises monthly averages from January through May, for the year 2003. This period was chosen to capture the development of the classical "blue hole" and the ensuing spring bloom in the Gulf of Lion area, and the somewhat more episodical development of an analogous, but much smaller, spring bloom in the Rhodes Gyre (see trends in Figure 3). The surface features recurring in these near-coastal hotspots

---

[1] QuikScat data are produced by Remote Sensing Systems and sponsored by the NASA Ocean Vector Winds Science Team. Data available at: http://www.remss.com/

[2] Source: National Aeronautics and Space Administration (NASA); SeaWiFS Ocean Reprocessing 5.1 (2005); for details see: http://oceancolor.gsfc.nasa.gov/REPROCESSING/SeaWiFS/R5.1/

[3] For the Levantine Basin, the two areas, for which the average wind speed and *Chl* values were calculated, are slightly displaced, in order to compensate for the displacement of the driving wind field and the Rhodes Gyre.

represent the main blooming events of the Mediterranean Sea, respectively in the western basin and in the eastern basin, that are not driven directly by continental (e.g. fluvial) runoff[4].

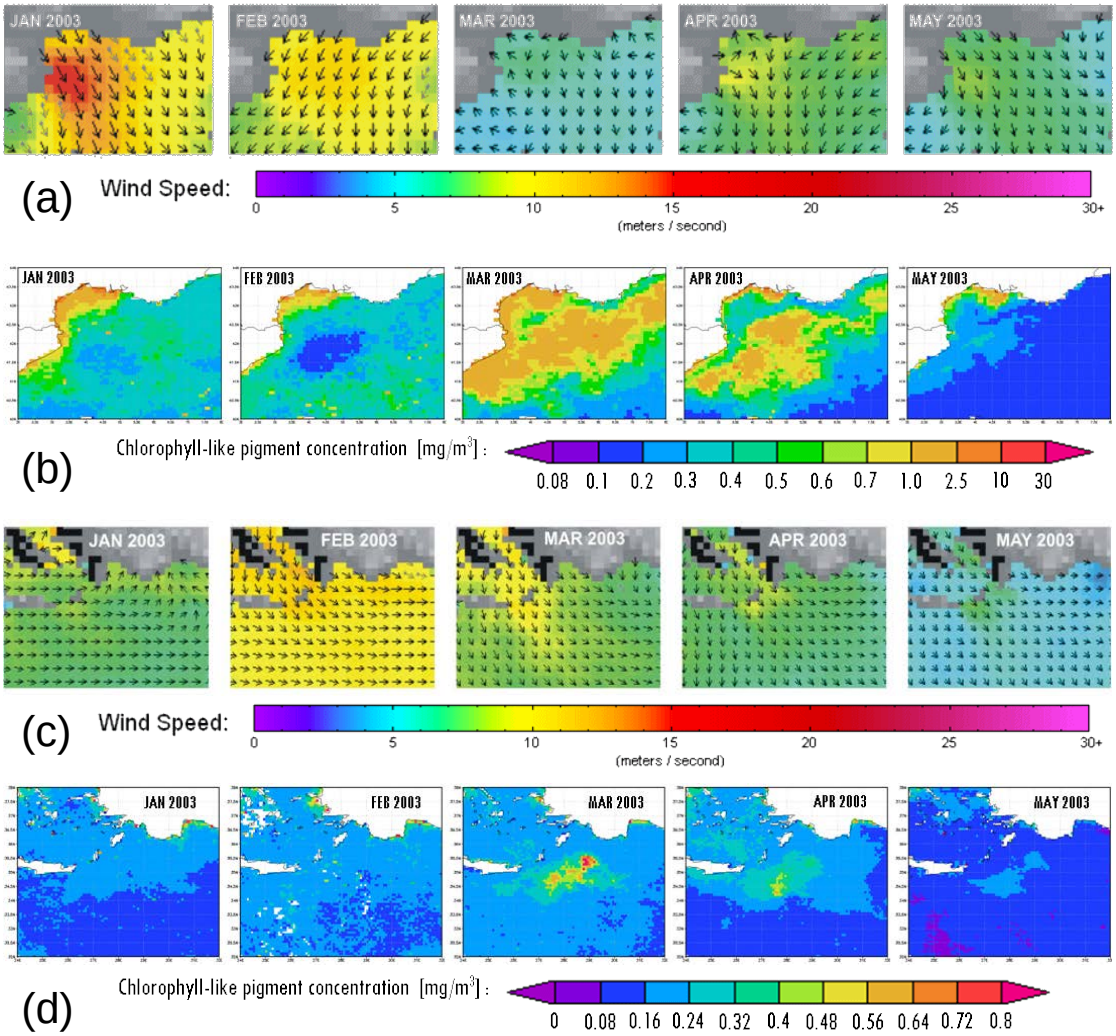

Figure 4: Monthly means, January to May 2003, of wind speed (panels a and c) and of Chl (panels b and d), in the Ligurian-Provençal Sea (panel a and b), February 2000, and in the Levantine Basin (panels c and d). The images cover the areas shown in Figure 1.

In the Ligurian-Provençal Sea, the highest wind speeds (around 10 m s^{-1}, or more) occur in January and February. This corresponds to low pigment concentrations (*Chl* < 0.5 mg m^{-3}), and often to the formation of a distinct "blue hole" (*Chl* < 0.2 mg m^{-3}), in the Gulf of Lion – although, at the monthly scale considered, the link is not always evident and unambiguous, in some of the years considered (not shown here). Lower wind speeds (between 5 and 10 m s^{-1}, or less), from March onwards, correspond to strong blooming (*Chl* > 1.0 mg m^{-3}).

A simple regression analysis, carried out using the entire 2000-2007 monthly mean values of the Ligurian-Provençal Sea (as plotted in Figure 3), is shown in Figure 5. Various time lags, from 0 to 6 months, were considered, in order to take into consideration the effect of two environmental factors: first, the biological response of the ecosystem cannot be instantaneous, after the set up of conditions favourable to algal growth (i.e. the increase in nutrient concentration due to vertical mixing); second, when the wind is strongest, the continuing deep convection can prevent blooming and lead instead to the formation of a "blue hole" in the pigment field. With no time lag (i.e. when the *Chl* values are matched with the wind speed of the same month; see Figure 5a), the linear fit shows essentially no correlation (R^2 ~ 0), while the second order polynomial fit (R^2 = 0.05) suggest that *Chl* is lower at lower wind speeds, and that it grows with wind speed, but only up to a point; then, as wind speed

[4] Note that the Rhone plume, in the Gulf of Lion area, presents separate dynamics.

becomes higher and higher, the *Chl* values drop again (i.e. corresponding to the occurrence of deep convection, see Figure 5b). As the time lag increases, so does the correlation. The maximum correlation is reached after 4 months (i.e. when the *Chl* values are matched with the wind speed of the 4 months before), with R^2 ~ 0.3 for both the linear and the polynomial fit. At higher time lags, the correlation decreases again to very low values (R^2 ~ 0.01, 0.02).

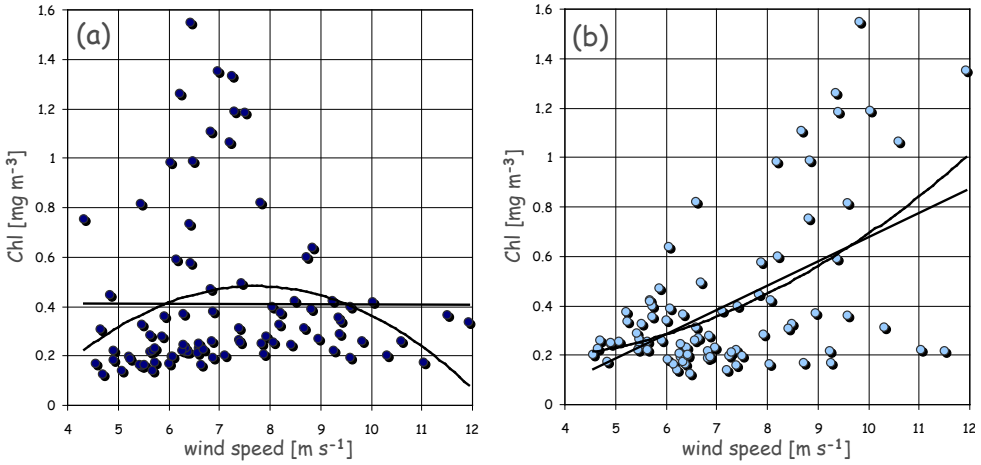

Figure 5: Regression analysis of monthly mean wind speed and Chl in the Ligurian-Provençal Sea, at two time lags, respectively of 0 (panel a) and 4 months (panel b).

The lack of a significant correlation, when wind speed and *Chl* are matched with no time lag, is due essentially to the fact that the ecosystem of the Ligurian-Provençal Sea responds in a very distinct manner to the extreme atmospheric forcing typical of winter months. In fact, if the regression analysis of monthly mean values is restricted to the first 4 months of the year, the correlation is more significant (R^2 ~ 0.28, both in the linear and in the polynomial case), but negative, as shown in Figure 6a. In this period, then, high *Chl* values occur only at lower wind speed. When the wind speed increases, and triggers the deep convection, the algae are mixed down to great depth in the water column, and cannot regain the surface to start over their photosynthetic activity. Conversely, for the remainder of the year, i.e. from May to December, the correlation is much lower (R^2 ~ 0.07, both in the linear and in the polynomial case), but positive, as shown in Figure 6b.

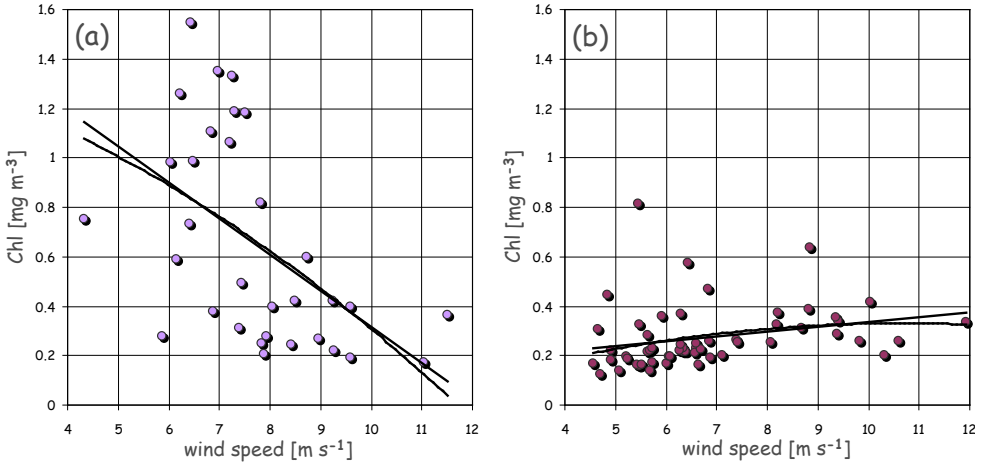

Figure 6: Regression analysis of monthly mean wind speed and Chl in the Ligurian-Provençal Sea, at 0 months time lag, for January to April (panel a) and May to December (panel b).

Somewhat weaker winds are measured in the Levantine Basin. Although the pattern is not as clear as in the Ligurian-Provençal Sea, wind speed is still higher in winter months (but well below the 10 m s^{-1} mark, in general), only to decrease slightly in spring months. Blooming events (*Chl* > 0.5 mg m^{-3}) in the Rhodes Gyre trail the periods of high wind speed. However, blooms just as intense as, if not more intense than, that of spring 2003 (see Figure 4), are

seen to occur also in other years, following winter months when the wind field did not present the same high values (ranging between 5 and 10 m s^{-1}).

The regression analysis, carried out using the entire 2000-2007 monthly mean values of the Levantine Basin, is shown in Figure 7. Once again various time lags were considered, this time mainly to take into consideration the delay of the biological response to the set up of conditions favourable to algal growth (since in this case the increase in nutrient concentration is essentially due to Ekman pumping within the cyclonic Rhodes Gyres, and not to sustained deep convection, continuing for long periods of time). With no time lag (*Chl* and wind speed of the same month; Figure 7a), both linear and polynomial fit show a positive correlation (with R^2 = 0.33 and R^2 = 0.35 respectively). The maximum correlation is reached with a time lag of 1 month (*Chl* matched to wind speed of the preceding month, Figure 7b), so that R^2 = 0.53 for both linear and polynomial fit. At higher time lags, the correlation decreases quickly to very low values, with R^2 ~ 0.3 at 2 months and R^2 ~ 0 at 4 months.

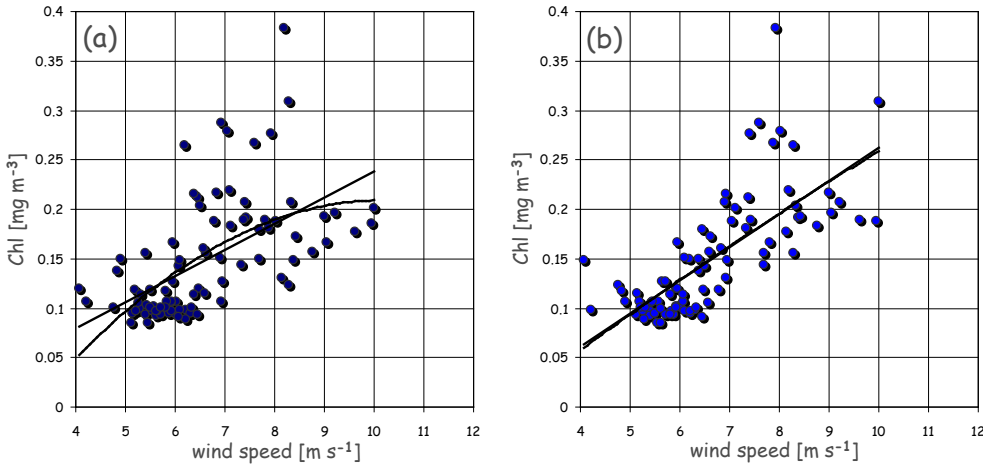

Figure 7: Regression analysis of monthly mean wind speed and Chl in the Levantine Basin, at two time lags, respectively of 0 (panel a) and 1 month (panel b).

Once again, the first 4 months of the year present a rather different situation, in the Levantine basin, as already seen for the Ligurian-Provençal Sea. The correlation is still low, in this period, when wind speed and *Chl* are matched with no time lag (R^2 = 0.03 in the linear case and R^2 = 0.13 in the polynomial case), but becomes much better with a time lag of 1 month (R^2 = 0.38 in the linear case and R^2 = 0.48 in the polynomial case), as shown in Figure 8a. From May to December, the correlation is high, both with no time lag (R^2 = 0.39 and R^2 = 0.51]) and with 1 month time leg (R^2 = 0.51 and R^2 = 0.55), as shown in Figure 8b.

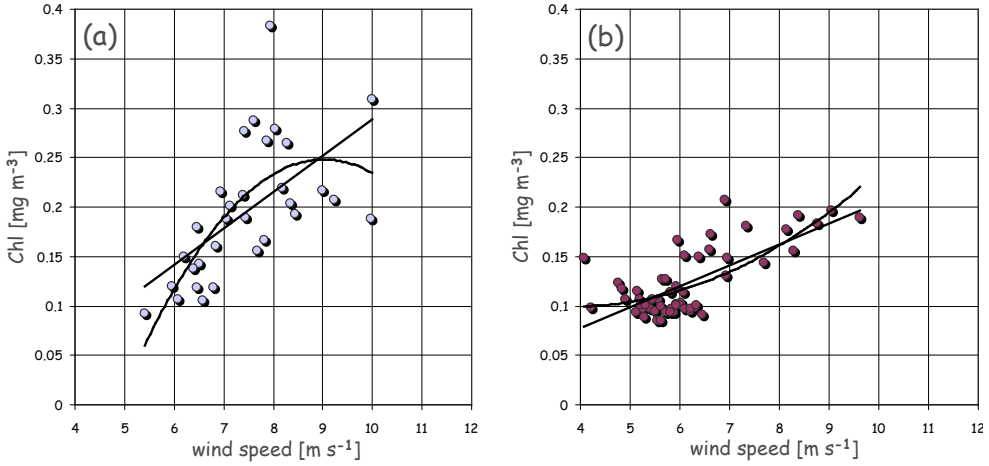

Figure 8: Regression analysis of monthly mean wind speed and Chl in the Levantine Basin, at 1 month time lag, for January to April (panel a) and May to December (panel b).

CONCLUSIONS

Algal growth in the Mediterranean Sea is always nutrient-limited, with consequent low biomass and primary production. The fertilization of the basin, supporting localized algal blooming, is ruled mainly by the impact of (coastal interactions and) atmospheric forcing in broad near-coastal zones, and then by the ensuing thermohaline processes.

In the Ligurian-Provençal Sea, the winter winds lead to convective processes that promote nutrient upwelling and then a sustained spring blooms, once the wind regime relaxes and surface stratification sets in. In the Levantine Basin, upwelling due to Ekman pumping, within the cyclonic component of the wind-generated Rhodes-Irapetra vortex pair, also results in similar, but weaker, algal blooms. However, other factors appear to be critical, in this second case (due to the different physical processes taking place), as the pattern of high wind regime followed by blooming has a much shorter time scale and does not recur systematically.

The examples presented here demonstrate that an improved interpretation of remote sensing data sets, and of the bio-geo-physical processes responsible for the observed phenomena, can be achieved through the combination of multi-sensor techniques. However, it is obvious that knowledge of the variability of pigment concentrations and surface winds is not sufficient for a full understanding of ecological dynamics in the two regions of interest.

Modeling of the correlation between *Chl* and wind speed, planned for the future development of this line of work, might be able to provide more clues on the coupling between algal blooms and wind patterns in the Mediterranean Sea. It should be noted, however, that much longer data sets, because would be required for a long-term analyses of the Mediterranean trends, particularly for the case of local changes in times of global warming.

REFERENCES

i. Barale V, 2005. Satellite observations as indicators of the health of the Mediterranean Sea. In: The Mediterranean Sea, edited by A Saliot (The Handbook of Environmental Chemistry, Vol 5 Water Pollution, Part K, Springer-Verlag, Berlin, Heidelberg), 387-408.

ii. Millot C. & I. Taupier-Letage, 2005. Circulation in the Mediterranean Sea. In: The Mediterranean Sea, edited by A Saliot (The Handbook of Environmental Chemistry, Vol 5 Water Pollution, Part K, Springer-Verlag, Berlin, Heidelberg), 31-66.

iii. Hamad N, C Millot & I Taupier-Letage, 2006). The surface circulation in the eastern basin of the Mediterranean Sea. Scientia Marina, 70(3): 457-503.

iv. Mélin F, B Bulgarelli, N Gobron, B Pinty & R Tacchi, 2000. An integrated tool for SeaWiFS operational processing (European Commission Publication no. EUR 19576 EN, Ispra, Italy) 34 pp..

v. Schroeder C, H Boggs, G Dome, M Halberstam, L Jones, J Pierson & J Wentz, 1982. The relationship between wind vector and normalized radar cross section used to derive Seasat-A satellite scatterometer winds. Journal of Geophysical Research, 87: 3318-3336.

vi. Donelan A & W J Pierson, 1987. Radar scattering and equilibrium ranges in wind-generated waves with application to scatterometry. Journal of Geophysical Research, 92: 4971-5029.

vii. Baith K, R Lindsay, G Fu & C R McClain, 2001. SeaDAS, a data analysis system for ocean-color satellite sensors. EOS Transactions AGU, 82: 202.

viii. Campbell J W, J M Blaisdell & M Darzi, 1995). Level-3 SeaWiFS Data Products: Spatial and Temporal Binning Algorithms. SeaWiFS Technical Report Series, Volume 32, NASA Technical Memorandum 104566. edited by S B Hooker, E R Firestone & J G Acker (NASA Goddard Space Flight Center, Greenbelt), 23 pp.